THEOS IMAGE RESTORATION USING OPTIMIZED HIGH-BOOST FILTER

Suphongsa Khetkeeree and Sompong Liangrocapart
Mahanakorn University of Technology, 140 Cheumsampan Rd,
Nongchock, Bangkok 10530, Thailand,
Email: suphongs@mut.ac.th, sompong@mut.ac.th

KEY WORDS: image restoration, high boost filter, MTF, NIIRS, THEOS

ABSTRACT: In this paper, we propose a novel method for satellite image restoration. This method base on high boost filter. The least square error condition is applied to optimize the boost coefficient of the high boost filter. Boost coefficient is arranged in an analytic form. Then its value can be computed directly from the formula. Thailand Earth Observation System (THEOS) panchromatic images are used to test the proposed method to retrieve original scenes. Modulation Transfer Function (MTF), Signal to Noise Ratio (SNR) and National Imagery Interpretability Rating Scale (NIIRS) are considered for image quality comparisons. The experimental results show that this method is superior to the traditional filter, e.g. Weiner filter, both vision and image quality metrics.

1. INTRODUCTION

When satellite sensor took a scene of the Earth, the original scene was degraded due to the physical properties of sensor optics, detectors, and electronics. The degradation phenomenon of the acquired images causes serious economic loss (Yang, L. et al., 2011). Thus, the image restoration in remote sensing field is an important task. It is one of the fundamental and longstanding problems in image processing community (Hanif and Seghouane, 2012). The objective of the restoration is to reconstruct an approximated version of the original image from a degraded observation (Dash, R. and Majhi, B., 2014).

Thailand Earth Observation Systems (THEOS) is major observation satellite of Thailand that launched in 2008. It has 2-m ground sampling distance (GSD) in panchromatic mode and 15-m GSD in multispectral mode. THEOS image is useful in many fields such as mapping, forestry management, disaster monitoring, land use planning etc.

In this work, a novel image restoration method is proposed. THEOS panchromatic imagery are used to test the model. Image quality of before and after restoration is verified and estimated quantitatively in terms of spatial image characterizations.

2. IMAGE DEGRADATION AND RELATED THEORY

2.1 Image Formation Model

The model of image formation can be shown as Figure 1. The resulting image is degraded by the imaging system. Let $g(x,y)$ is a degraded image which is produced from the degradation of imaging system on an original scene, $f(x,y)$. The degradation of an image can separate into two parts as blurring and additive noise. Optical instruments, atmosphere, sensor and moving of imaging system often are the causes of blurring in the images while the incident of photons on the sensor and the electronics are the causes of additive noise.

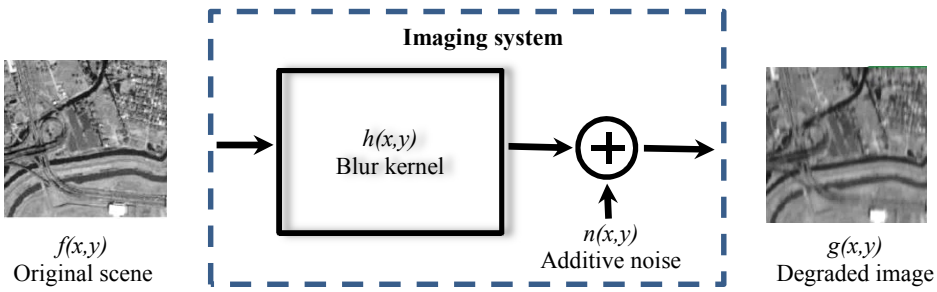

Figure 1. A model of image formation.

If $h(x,y)$ be the blur kernel which is also known as the point spread function (PSF) (Aouinti et al., 2016). Let $n(x,y)$ is an additive noise of the imaging system and a blur kernel is linear and spatially invariant, then the image degradation model in spatial domain can express as

$$g(x,y) = h(x,y) \otimes f(x,y) + n(x,y) \tag{1}$$

where $\otimes$ is the convolution operator.

2.2 High Boost Filter

A high boost filter is one of high pass filters. The general usability of this filter is often employed for sharpening the image detail and enhancing the high frequency component. From the general definition of high boost filter can be written as

$$g_{HB}(x,y,b) = g(x,y) + b \cdot \mathrm{HP(x,y)} \otimes g(x,y), \;\; b \geq 0 . \tag{2}$$

When g_{HB} is a resulting image when an image $g(x,y)$, is filtered by a high boost filter, $\mathrm{HP(x,y)}$ is a high pass filter and a constant *b* is a boost coefficient. If a high boost filter can restore the degraded image and let $\hat{f}(x,y)$ is a restored image, the formula for restoring image by high boost filter can be shown as below equation.

$$\hat{f}(x,y,b) = g(x,y) + b \cdot \mathrm{HP(x,y)} \otimes g(x,y), \;\; b \geq 0 \tag{3}$$

2.3 Bilateral Filter

In the image formation model, the additive noise is a high frequency component, thus an image restoration by high boost filter is strong noise amplification. In other word, this restoration can apply in the case which ignores an additive noise. However, most imaging systems always have a noise, thus the restoration by high boost filter needs the prior process to reduce an additive noise and this process does not change the blur kernel because the detail in an image is disappeared. The bilateral filter is one of the reducing noise filter which has property for suppressing an additive noise and preserving the high frequency component. This filter is proposed by Tomasi and Manduchi (Tomasi and Manduchi, 1998) which can be written as

$$g^{b}_{i,j} = \frac{1}{w_{i,j}} \sum_{k=-M}^{M} \sum_{l=-N}^{N} g_{i+k,j+l} d_{k,l} \, r_{k,l} \; . \tag{4}$$

Where g^{b} is the resulting image by bilateral filter, g is a degraded image that has an additive noise and w is a normalized term. d and r terms are a domain filter and a range filter in $(2\mathrm{M}+1)\times(2\mathrm{N}+1)$ mask, respectively.

2.4 Traditional Image Restoration for Image Comparison

In this paper, we used the Weiner filter (Gonzales and woods, 1992) to compare the proposed method.This filter is popularly used to restore the remote sensing images (Yang et al., 2011, Aouinti et al., 2016). It can formulate as

$$\hat{f}(x,y) = \mathscr{F}^{-1}\left\{ \frac{H^{*}G}{|H|^{2} + k} \right\} \tag{5}$$

where H and G are the frequency domain of $h(x,y)$ and $g(x,y)$, respectively, while $\mathscr{F}^{-1}\{\;\}$ is the inverse Fourier transform and $*$ denotes the complex conjugate. A parameter *k* is a noise power spectrum, which it is difficult to estimate it. If the value of *k* is too high, then the restored image is too blurred, on the other hand, if the value of *k* is too low, then the noise is too amplified. For this comparison, we use the least square error condition to estimate the value of parameter *k*.

2.5 Least Square Error Condition

This condition is main used in this paper, if the restored image as $\hat{f}(x,y)$ and the original image as $f(x,y)$, an error of each pixel can express as $e(x,y)=f(x,y)-\hat{f}(x,y)$, but in fact, a $f(x,y)$ is not available. Hence, the convolution by a blur kernel is employed to estimate the square error. If the noise in image degradation model is ignored, the square error can formulate as

$$\|e(x,y)\|_2^2=\left\|g(x,y)-h(x,y)\otimes\hat{f}(x,y)\right\|_2^2 \tag{6}$$

The least square error or the minimum square error is an algorithm which can determine the parameter in a restoration process that gives the minimum value of the square error. For example, we apply this condition to estimate a parameter *k* of a Weiner filter, that is

$$k=\min_k\left\|g(x,y)-h(x,y)\otimes\hat{f}(x,y,k)\right\|_2^2 \tag{7}$$

where $\hat{f}(x,y,k)$ presents the restored image by a Weiner filter. The parameter *k* is searched for a case that has minimum of the square error.

3. PROPOSED WORK

3.1 Optimization of Boost Coefficient

Behaviour of a high boost filter can show in Figure 2. When the boost coefficient is a small value, the restored step edge from the degraded version is small sharpening. However, if the boost coefficient is a large value, the restored edge is higher sharpened and it has very high of the edge overshoot. The sharpest of restored edge and the lower of the edge overshoot is needed to approach the image restoration.

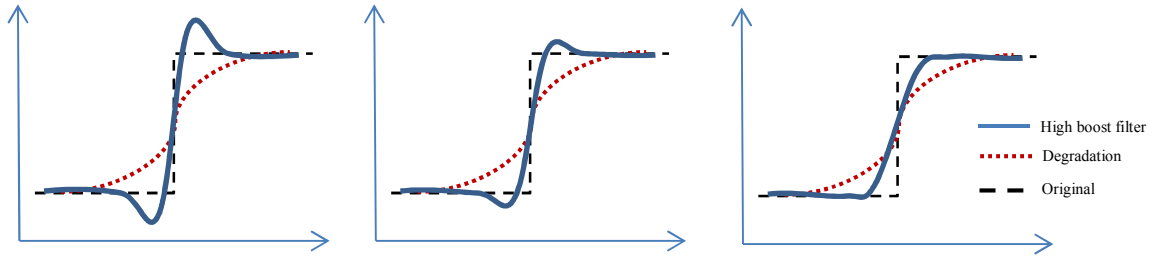

(a) (b) (c)

Figure 2. The effect of a boost coefficient on the degraded-step edge, (a) large boost coefficient, (b) exactly boost coefficient, (c) small boost coefficient.

In the case that noise is ignored, we can determine the optimization of the boost coefficient by using the least square error condition. This condition can be written as

$$b=\min_b\left\|g(x,y)-h(x,y)\otimes\hat{f}(x,y,b)\right\|_2^2 \tag{8}$$

Where $\hat{f}(x,y,b)$ is a restored image by the high boost filter in equation (3). The optimized boost coefficient can define by substitute equation (3) into the equation (8), and differentiate the square error function by *b* as zero. The solution of this optimization can express as.

$$b=\frac{\|g(x,y)-h(x,y)\otimes g(x,y)\|_2}{\|h(x,y)\otimes HP(x,y)\otimes g(x,y)\|_2} \tag{9}$$

3.2 Design of Bilateral Filter

A domain filter common is a low pass filter for reducing the additive noise, but a weight of this filter depends only on distance of pixels. The range filter is used to adjust the weight of a domain filter. To preserve the edge (blur kernel), the range filter is more weight in the case that small difference of radiometric and it is less weight when the radiometric has large different. The Gaussian distribution is popular and reasonable function for applying to the range filter and the domain filter of a bilateral filter, which can write as

$$r_{k,l} = \exp\left(-\left(\frac{\left(g_{i,j} - g_{i+k,j+l}\right)^2}{2\sigma_r^2}\right)\right) \quad \text{and} \quad d_{k,l} = \exp\left(-\left(\frac{k^2}{2\sigma_x^2} + \frac{l^2}{2\sigma_y^2}\right)\right) \tag{10}$$

where σ_x, σ_y and σ_r is the standard deviation of a domain filter (subscript x, y denote the across track and the along track) and range filter, respectively.

4. EXPERIMENTS

In this section, we demonstrate a region of interest that use in this experiment and describe the summary of parameter that use for comparison. After that, the methodology of this experiment is described.

4.1 Region of Interest

The THEOS imagery at Salon de Provence, France (43.605916N, 5.120188E) were used in this experiment because this scene (Figure 3) has the remote sensing target which it can estimate the spatial characteristic and image quality for compare the proposed method. We separate the area in the remote sensing target as the Figure 4. . The 1-4 regions are employed for estimating the edge response while the 5-6 regions are applied to compute the SNR. The ESF is the fundamental function which can apply to estimating the MTF and the NIIRS.

Figure 3. The remote sensing target in the airport at Salon de Provence, France.

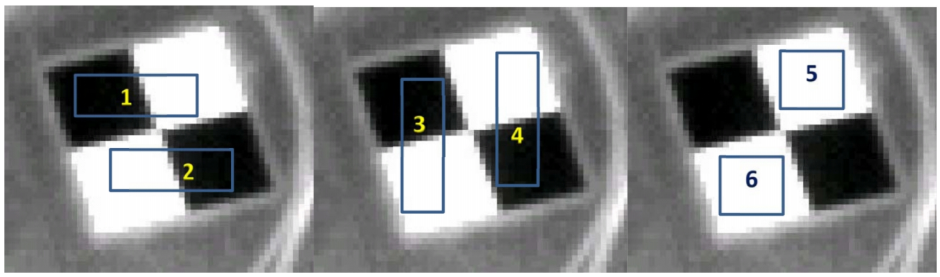

Figure4. The region of interest in the remote sensing target, area 1-4 are used to construct the edge response and area 5-6 are employed to estimate the signal to noise ratio.

4.2 Parameter for Comparison

We use popular three parameters of spatial characteristics and image quality, which are the signal to noise ratio (SNR), modulation transfer function (MTF) and National Image Interpretability Rating Scale (NIIRS). The brief definition of these parameters is presented in the next subsection.

4.2.1 SNR Estimation: We estimate the SNR for this experiment by using laboratory methods. The SNR is the ratio of the mean (μ) and the standard deviation (σ) in homogeneous areas. That is

$$SNR = \frac{\mu}{\sigma} \tag{11}$$

If digital number of image intensity can replace it by DN. The mean and standard deviation of a digital image is given by following equation.

$$\mu = \frac{1}{N}\sum_{i=1}^{N} DN_i \qquad \text{and} \qquad \sigma = \sqrt{\frac{1}{N-1}\sum_{i=1}^{N}\left(DN_i - \sigma\right)^2} \tag{12}$$

When N is a number of pixels in the selected area.

4.2.2 MTF Estimation: The ESF of 1-2 regions and 3-4 regions in Figure 4 are used to estimate the across MTF and along MTF, respectively. The MTF is the magnitude of the point spread function (PSF) in the frequency domain. The line spread function (LSF) is the 1dimension of the PSF, which can estimate from differential of the ESF. The process for obtaining the MTF can show in Figure 5. The MTF at Nyquist frequency is popularly used to represent the limits of MTF which can define at half of normalized spatial frequency.

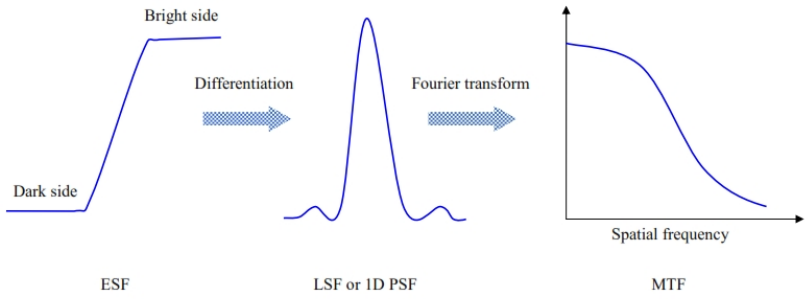

Figure 5. The process for estimating the MTF

4.2.3 NIIRS Estimation: The NIIRS is overall quality metrics that has 10-level (0-9). Each level of the NIIRS is defined by the criterion of the Imagery Resolution Assessments and Reporting Standards (IRARS) (IRARS, 2016). The other way of estimating the NIIRS is a General image equation (GIQE), which it is composed by many characteristics such as ground sampled distance (GSD), relative edge response (RER), SNR and edge overshoot. The GIQE has many versions, but 4th version is popular. This version is the empirical formula, which developed by Leachtenauer et al. The formula can be written as follow equation.

$$\text{NIIRS} = 10.251 - a\log_{10}\text{GSD}_{\text{GM}} + b\log_{10}\text{RER}_{\text{GM}} - 0.656\text{H}_{\text{GM}} - 0.344\text{G/SNR} \tag{13}$$

Where GSD_{GM} is the geometric mean of a ground sampled distance that computes in inches, RER_{GM} is the geometric mean of the relative edge response, H_{GM} is the geometric mean of edge overshoot, G is the noise gain of MTF compensation kernel and SNR is the signal to noise ratio. The constants a and b are equal 3.32 and 1.559, respectively, if $\text{RER}_{\text{GM}} \geq 0.9$, and they are equal 3.16 and 2.817, respectively, if $\text{RER}_{\text{GM}} < 0.9$.

A normalized edge response is obtained from the normalization of the ESF. The RER is an absolute different value of a normalized edge response at ± 0.5 pixel from the edge while the H is estimated from the highest of the edge overshoot over 1-3 pixels from the edge which it can show in Figure 6.

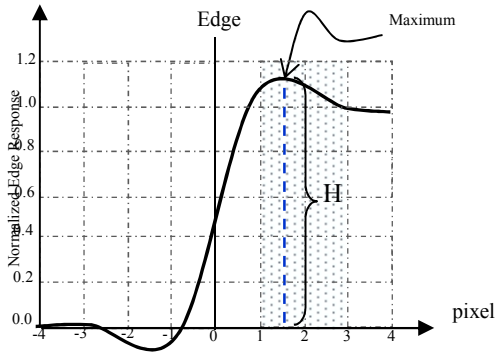

Figure 6. The definition of the edge overshoot

The SNR is estimated from the ratio of the noise of the dc differential scene radiance to the noise of the rms electrons that compute before the MTF compensation and after calibration. The noise of the dc differential scene radiance is the difference in detector output at 7% and 15% reflectance of Lambertian surfaces (Ryan et al., 2003). However, we use the laboratory method (see subsection of the SNR estimation) for estimating the SNR because it is convenient and this quantity is least effect (Li et al., 2014) to the NIIRS estimation.

A parameter, G is the noise gain, which define from the restored filter that is not normalized. The definition of the noise gain is formulated as

$$G = \sqrt{\left(\sum_{i=1}^{M} \sum_{j=1}^{N} \left(w_{i,j} \right)^2 \right)} . \tag{14}$$

Where w is the $M \times N$ mask restored filter.

4.3 Methodology

For convenience of discussion, the first filter, which only is the optimized high boost filter, is assigned as OHBF and the second filter, which use the bilateral filter before restoration by the optimized high boost filter, is assigned as BOHBF while the optimized Weiner filter is assigned as OWF.

In the first experiment, three filters are applied to THEOS images, after that the restored images of each method are compared with the spatial characteristics and image quality (SNR, MTF at Nyquist and NIIRS). For last experiment, we apply the optimized boost coefficient of this scene to another scene which has the same target, but not same time. The optimized Weiner filter is used to compare again, however the PSF in the Weiner filter use the same scene with the scene that used to estimate a boost coefficient.

5. RESULTS AND DISCUSSION

The scene in Salon de Provence, France on August 15, 2009 is applied in the first experiment. A Figure 7 shows the vision results of the original image (a), the OWF (b), and both proposed methods ((c) is OHBF, (d) is BOHBF). The quality metrics (across MTF at Nyquist (MTFx), along MTF at Nyquist (MTFy), SNR and NIIRS) of each method are presented in Table 1. The result of both proposed method are better than the OWF. Moreover, image quality metrics results of the BOHBF are superior than other methods. However, the SNR of the OHBF is lower than the OWF because the OHBF has not the reducing noise filter. The vision of both proposed methods sharpens than the OWF. The vision of the OHBF is very obvious in a detail of the restored image, but it has a lot of the noise.

Table 1. The experimental results of the spatial characteristics and image quality

Method	**MTF_x**	**MTF_y**	**SNR**	**NIIRS**
Original	0.111	0.240	95.8	2.831
OWF	0.489	0.780	60.6	3.238
OHBF	0.845	0.928	43.5	3.403
BOHBF	0.868	0.938	67.5	3.421

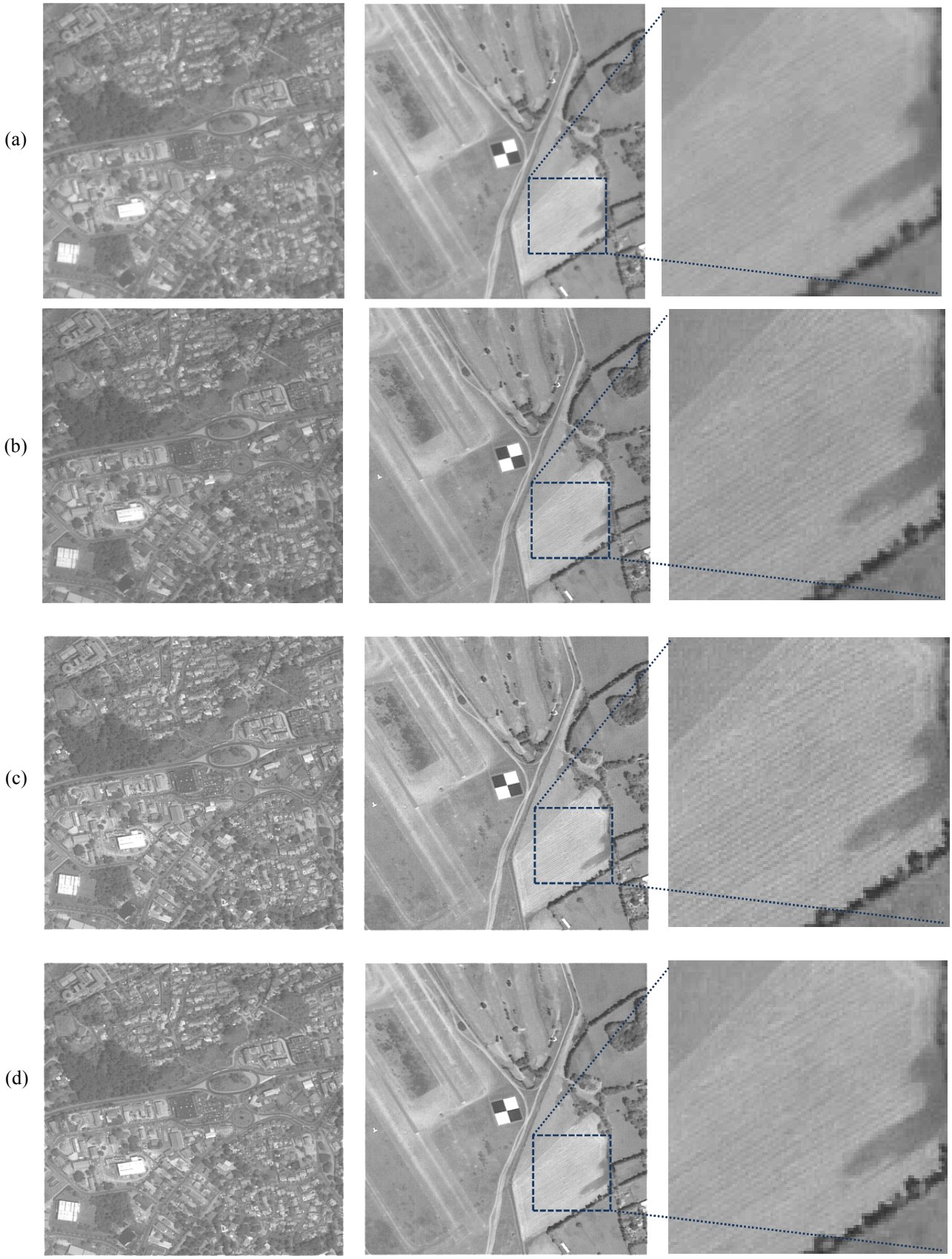

Figure 6. The stretching images of (a) the degraded image (raw data) and the resulting image from, (b) OWF, (c) OHBF and (d) BOHBF. The small picture on right side is 4x zoom of the large picture on the center.

The results of second experiment are presented in the Table 2. In this experiment, the boost coefficient from scene on August 15, 2009 is applied to the other scene. Both proposed methods are superior to the OWF, but not include the signal to noise ratio. The signal to noise ratio of BOHBF is small differences from the OWF which is not significant, however the OHBF is large different because this filter is not the reducing noise filter.

Table 2. The image quality metrics of both proposed methods when using the boost coefficient of scene on August 15, 2009 to other scene and the optimized Weiner filter when using the same PSF of scene on August 15, 2009.

Date	Method	MTFx	MTFy	SNR	NIIRS
Mach 29, 2012	Original	0.110	0.241	86.2	2.826
	OWF	0.535	0.807	60.1	3.261
	OHBF	0.862	0.929	49.1	3.415
	BOHBF	0.867	0.932	58.6	3.419
June 17, 2015	Original	0.096	0.227	59.2	2.809
	OWF	0.441	0.736	45.2	3.201
	OHBF	0.828	0.927	38.4	3.405
	BOHBF	0.834	0.928	43.3	3.409

6. CONCLUSIONS

In this paper, a novel image restoration method of THEOS panchromatic imagery is proposed. A high boost filter is applied to restore a degraded image. The least square error condition is applied to optimize the boost coefficient of the high boost filter. Boost coefficient is arranged in an analytic form. Then it can be computed directly from its formula. For a better result, the bilateral filter is used to suppress the additive noise before the restoration process by an optimized high boost filter. THEOS images at Salon de Provence in France are used in our experiment. Results show that the sharpness of the image can be restored. High image quality can be achieved. In another method comparison, the proposed method is superior to Weiner filter, both vision and image quality metrics. This method may also be applied to other imaging system.

7. REFERENCES

Aouinti, F., Nasri, M. Moussaoui, M., Benchaou, S., and Zinedine, K., 2016. Satellite image restoration by applying the genetic approach to the Weiner deconvolution. 13th International conference computer graphics, imaging and visualization.

Dash, R. and Majhi, B., 2014. Motion blur parameters estimation for image restoration. Optik-International Journal for Light and Electron Optics, vol. 125, no. 5, pp. 1634-1640.

Gonzalez, R.C., and Woods, R.E., 1992. Digital Image Processing., Addison-Wesley Publishing Company, Inc., London, UK.

Hanif, M., and Seghouane, A., 2012. Blurred image deconvolution using Guassian scalar mixtures model in wavelet domain. 2012 International conference on digital image computing techniques and applications (DICTA).

Imagery Resolution Assessment and Reporting Standards (IRARS) Committee., 2016. Civil NIIRS Reference Guide. Retrieved August 16, 2016, from: http://fas.org/irp/imint/niirs_c /app2.htm

Leachtenauer, C.J., Malila, W., Irvine, J., Colburn, L. and Salvaggio, N., 1997. General image-quality equation: GIQE. Applied Optics, vol. 36, pp. 8322-8328.

Li, L., Luo, H., and Zhu, H., 2014. Estimation of the interpretability of ZY-3 sensor corrected panchromatic nadir data**.** Remote Sense, vol.6, pp. 4409-4429.

Ryan, R., Baldridge, B., Schowengerdt, R.A., Choi, T., Helder, D.L. and Blonski, S., 2003. IKONOS spatial resolution and image interpretability characterization. Remote sensing of environment, vol.88, pp. 37-52.

Schowengerdt, R.A., 2007. Remote sensing: models and methods for image processing 3rd editon. Elsevier Inc, London, UK, pp. 234-235.

Tomasi, C. and Manduchi, R., 1998. Bilateral filtering for gray and colour image. Proceeding of the IEEE international conference on computer vision, Bombay, India, pp. 839-846.

Yang, L., Zhang, X. and Ren, J., 2011. Adaptive Weiner Filtering with Gaussian Fitted Point Spread Function in Image Restoration. In Proceeding of the 2011 IEEE 2nd International Conference on Software Engineering and Sevice Science (ICSESS), Beijing, Chaina, 15-17 July 2011, pp. 890-894.